31st Annual International Conference of the IEEE EMBS
Minneapolis, Minnesota, USA, September 2-6, 2009

A Two-Equation Coupled System Model for Determination of Liver Tissue Temperature during Radio Frequency Ablation

D. P. O'Neill, T. Peng, S. J. Payne
Department of Engineering Science, University of Oxford, UK

***Abstract*— A model is presented that is an alternative approach to the bio-heat equation for use in radio frequency heating of the liver. The model comprises both a tissue subvolume and a blood subvolume. Separate bio-heat equations are determined for each subvolume, but with an additional term exchanging heat between them, thus creating a coupled system. The derivation for the two coupled differential equations is outlined and sample simulations are presented to demonstrate the importance of considering the two subvolumes separately, even when the blood subvolume is a small fraction of the tissue subvolume.** [1]

I. INTRODUCTION

Dissection of tumours is often the chosen therapy for hepatocellular carcinoma, but about 75% of patients cannot be treated solely by dissecting tumours. In contrast to resection, radio frequency ablation (RFA) is a minimally invasive treatment and can be performed percutaneously. However, this form of therapy still has major drawbacks: the exact extension of the necrosis zone is almost impossible to plan or monitor and assessment of the results during or right after the procedure is very limited.

A bottleneck on the way towards the patient specific planning tool is our limited understanding of processes during tissue heating and, ultimately, tissue death as the result of that heating. The established bio-heat equation as described by Pennes [6] does not match with experimental data in liver tissue and there exists no validated simulation of a real situation.

Models derived from continuum approximations have previously been proposed – see review papers [1], [2], [4] – as well as models based on specific vessel architecture – [7], [8]. Chen and Holmes [3] propose a model based upon two subvolumes, but the analysis yielded a single analytic equation.

We therefore present in this paper a more realistic physiological model of the heat generation and transfer processes, which will enable us to compare our predictions with experimental data more easily.

II. THEORY

A. Derivation of heat equations

The model is based upon conservation of energy in an arbitrary control volume. Equation (1) shows the considered heat terms for the control volume where ρcV is the heat capacity of the control volume, Q^{cond} and Q^{bulk} are the net heats leaving the control volume via thermal conduction and via bulk blood flow respectively, whilst Q^{RFA} and Q^{m} are the heats generated in the control volume due to radio frequency heating and due to metabolic processes.

$$\rho cV\frac{\partial T}{\partial t} = V\left(-Q^{cond} - Q^{bulk} + Q^{RFA} + Q^{m}\right) \qquad (1)$$

By considering the control volume as two subvolumes – one consisting of the blood present in the control volume, V_b, and one consisting of tissue, V_t – and by including a new term, Q^{tb}, to account for the heat transferred from the tissue subvolume to the blood subvolume, (1) can be rewritten as two coupled equations (2) and (3):

$$\rho_t c_t\frac{V_t}{V}\frac{\partial T_t}{\partial t} = -Q_t^{cond} + Q_t^{RFA} + Q_t^{m} - Q^{tb} \qquad (2)$$

$$\rho_b c_b\frac{V_b}{V}\frac{\partial T_b}{\partial t} = -Q_b^{cond} - Q_b^{bulk} + Q_b^{RFA} + Q_b^{m} + Q^{tb} \qquad (3)$$

$$\frac{V_t}{V} + \frac{V_b}{V} = 1 \qquad (4)$$

Using the assumption that all mass within the control volume is accounted for by one of the the two subvolumes, (4), (2) and (3) sum together to form (1).

B. Heat Equation Components

Q^{cond} accounts for the transfer of thermal energy between neighbouring molecules in a particular subvolume due to the local temperature gradient for that subvolume. For the heat equations in the model, Fourier's Law for heat conduction is used:

$$Q = kA\nabla T,$$

where k is the thermal conductivity and A is the surface area over which the conduction takes place. Thus, for use in (1), the constitutive equation in differential form, is:

$$Q^{cond} = -V\nabla\cdot\left(k\nabla T\right). \qquad (5)$$

[1]The research leading to these results has received funding from the European Community's eventh Framework Programme under grant agreement n° 223877, project IMPPACT.

During radio frequency heating, the source term Q^{RFA} is present. The magnitude of the of heating is determined by the electric field generated by the ablation probe, and is calculated from:

$$Q^{RFA} = V\sigma \left|\nabla\varphi\right|^2, \tag{6}$$

where σ is the electrical conductivity and ϕ is the electric potential.

As the proposed model is designed for the purpose of calculating liver temperature in regions undergoing RFA treatment, the source term accounting for the heat generated during metabolic processes is negligible in comparison to Q^{RFA}. Thus:

$$Q^m \approx 0. \tag{7}$$

By continuing the concept of considering separate subvolumes and considering the well-perfused state of the liver, mass will be continuously flowing through the blood subvolume. The proposed model approximates the liver to a porous medium with flow obeying Darcy's Law such that the volume flux $\vec{u}$ is given by:

$$\vec{u} = -\frac{\kappa}{\mu}\nabla p, \tag{8}$$

where κ is the permeability of the medium, μ is the dynamic viscosity of the fluid and P is the pressure. The bulk flow heat term, Q^{bulk}, accounts for the heating leaving the control volume as heated blood and is calculated from:

$$Q^{bulk} = \rho_b c_b \left(\nabla T_b \cdot \vec{u}\right). \tag{9}$$

The final term, Q_{tb}, considers the heat transferred from the tissue subvolume to the blood subvolume via convection and thereby links the two subvolumes and forms a coupled pair of equations. Equation (10) equates the heat transfered convectively as proportional to the difference between the tissue and blood subvolumes temperatures. Due to modeling the liver as a porous medium, the exact flow regime and total blood vessel surface area are both unknown. Without this knowledge, the form of forced convection cannot be determined and therefore the heat transfer coefficient h is unobtainable from standard results. The constant of proportionality, $(hA)_{tb}$, accommodates for both unknowns: the heat transfer coefficient and the unmodeled vessel surface area.

$$Q^{tb} = (hA)_{tb}\left(T_t - T_b\right) \tag{10}$$

C. Expanded Heat Equations

Substituting (5), (6), (7), (8), (9) and (10) with appropriate subvolume subscripts into (2) and (3) gives the expanded heat equations:

$$\rho_t c_t \frac{V_t}{V}\frac{\partial T_t}{\partial t} = V_t\nabla\cdot(k_t\nabla T_t) + V_t\sigma_t\left|\nabla\varphi\right|^2 - (hA)_{tb}\left(T_t - T_b\right) \tag{11}$$

$$\rho_b c_b \frac{V_b}{V}\frac{\partial T_b}{\partial t} = V_b\nabla\cdot(k_b\nabla T_b) + \rho_b c_b\left(\nabla T_b\cdot -\frac{\kappa}{\mu}\nabla p\right) + V_b\sigma_b\left|\nabla\varphi\right|^2 + (hA)_{tb}\left(T_t - T_b\right) \tag{12}$$

D. Precursor Equations

Before solving (11) and (12) p and φ need to be determined.

Continuity of mass applies to any arbitrary control volume thus,

$$\nabla\cdot(\rho_b\vec{u}) = 0,$$

and assuming that blood is incompressible,

$$\nabla\cdot\vec{u} = 0. \tag{13}$$

Substituting (8) into (13) gives

$$\nabla\cdot\left(-\frac{\kappa}{\mu}\nabla p\right) = 0,$$

which, by modeling the whole liver as well perfused and assuming the blood has constant viscosity can be further simplified to

$$\nabla^2 p = 0, \tag{14}$$

which is easily solvable given boundary conditions.

An analogous approach to electric potential yields

$$\nabla^2\varphi = 0. \tag{15}$$

E. Implementation Steps

In preparation for numerical simulations, it is necessary to set boundary conditions for solving (14). The way set out in the proposed model is to create an array containing 1 for any point that exists in a vessel on the arterial side of the network, -1 for any point that exists in a vessel on the venous side of the network, and 0 otherwise. The pressure array can then be initialised by mapping the vessel network array and assigning a positive pressure and a negative pressure in the pressure array to the values 1 and -1 in the vessel network array. The whole array is then linearly adjusted such that the minimum pressure anywhere is 0. The difference in pressure is determined by the user, but the authors suggest a pressure relating to difference between mean arterial pressure and central venous pressure. Any points on the surface of the array are kept at their initialised pressure.

In order to generate numerical simulation results, the proposed model is designed to be implemented by proceeding through the following steps:

1) Set Vessel Network Array
2) Initialise Pressure Array
3) Solve (14) to obtain pressure array
4) Solve (15) to obtain potential difference array
5) Initialise Blood Temperature and Tissue Temperature arrays
6) Solve (11) and (12) to obtain temperature arrays

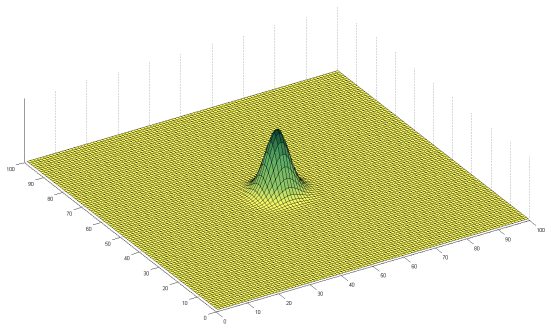

Fig. 1: Plot of Gaussian heat source used to replace RF heating source term in simulations

Parameter and Description	Value and Unit
ρ_t, tissue density	$1060kgm^{-3}$
ρ_b, blood density	$1060kgm^{-3}$
c_t, tissue specific heat capacity	$3600Jkg^{-1}K^{-1}$
c_b, blood specific heat capacity	$4180Jkg^{-1}K^{-1}$
k_t, tissue termal conductivity	$0.49Wm^{-1}K^{-1}$
k_b, blood termal conductivity	$0.49Wm^{-1}K^{-1}$
$\frac{V_b}{V}$, blood volume fraction	$0.02m^0$
$(hA)_{tb}$, heat transfer coefficient	$10000.49Wm^{-3}K^{-1}$
κ, porosity	$0.02m^2$
μ, dynamic viscosity	$3.1 \times 10^{-3}kgm^{-1}s^{-1}$

TABLE I: Parameters used in the model simulations

III. Simulation Results

The model described in the previous section can now be used in the preceding implementation steps to produce various temperature profiles over time in an sample of modeled liver under RF heating.

For simplification of numerical analysis all tissue properties are assumed to be homogeneous and isotropic. Properties are modeled as invariant with temperature, pressure and electric potential.

For ease of displaying simulation results here, all simulations are two-dimensional, plotted on a square array of 100x100 data points. Further, to best demonstrate the effect on temperature profile development caused by using the coupled equation approach, the precursor equations were simplified by setting not solving (15) but rather setting Q^{RFA} to a Gaussian heat source centered on point (50,50) as shown in Fig. 1.

The vessel network array used for the simulations contained one artery and one vein. The artery was located centered on point (80,80) and the vein at point (30,30), resulting in a symmetrical simulation. Both were of equal area – 10x10 – thereby observing continuity of mass for the area considered. Fig. 2 shows the Vessel Network as defined by the authors for use in simulations.

Fig. 3 shows the resulting pressure distribution after Fig. 2 was used for the boundary conditions in solving (14).

The simulation discussed hereon runs in simulation time from 0 - 5000 in unit time increments. For the simulation, the heat source was active for a duration of 90 time increments – between time steps 10 and 100. Table I presents the values and units used in the simulations.

A selection of snapshots are shown in Fig. 4 with the Tissue Temperature fields on the top, and Blood Temperature fields below. The left hand pair show the fields at simulation time 50, followed by times 200, 1000 and 5000.

IV. Discussion

The tissue temperature field at time 50 clearly follows the Gaussian heating as no bulk flow field distortion effect has started. Evidence of distortion is visible in the Blood Temperature field at time 200. However, due to the low volume fraction of the blood subvolume, $\frac{V_b}{V}$, of 0.02, the thermal mass of the blood is low and the effect on the tissue subvolume is not obvious at time 200. Slight distortion of the Tissue Temperature field is displayed at time 1000, but it is clear at time 5000, where the field appears similar to the Blood Temperature field displayed at time 1000. In simulations run with closer matched subvolumes the thermal lag exhibited here is lessened. The thermal lag is thus significant, even for a very small blood volume fraction (2%).

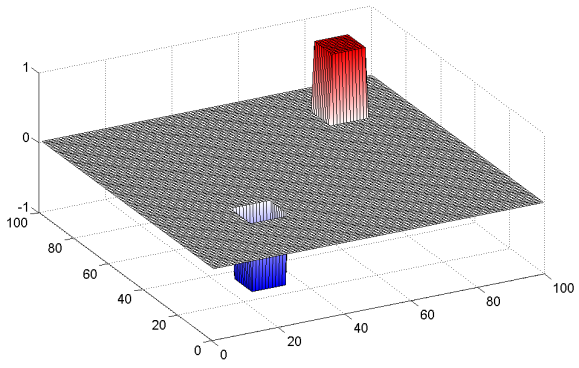

Fig. 2: Vessel Network used in simulations

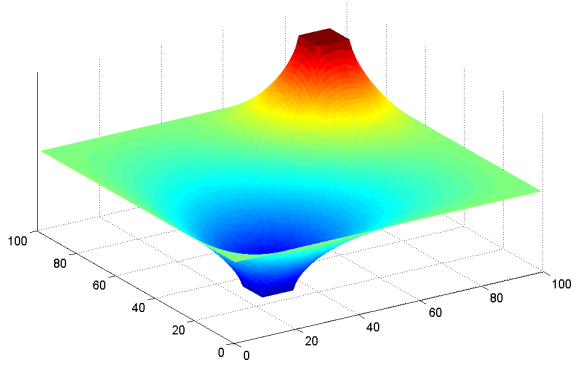

Fig. 3: Pressure distribution calculated for simulations

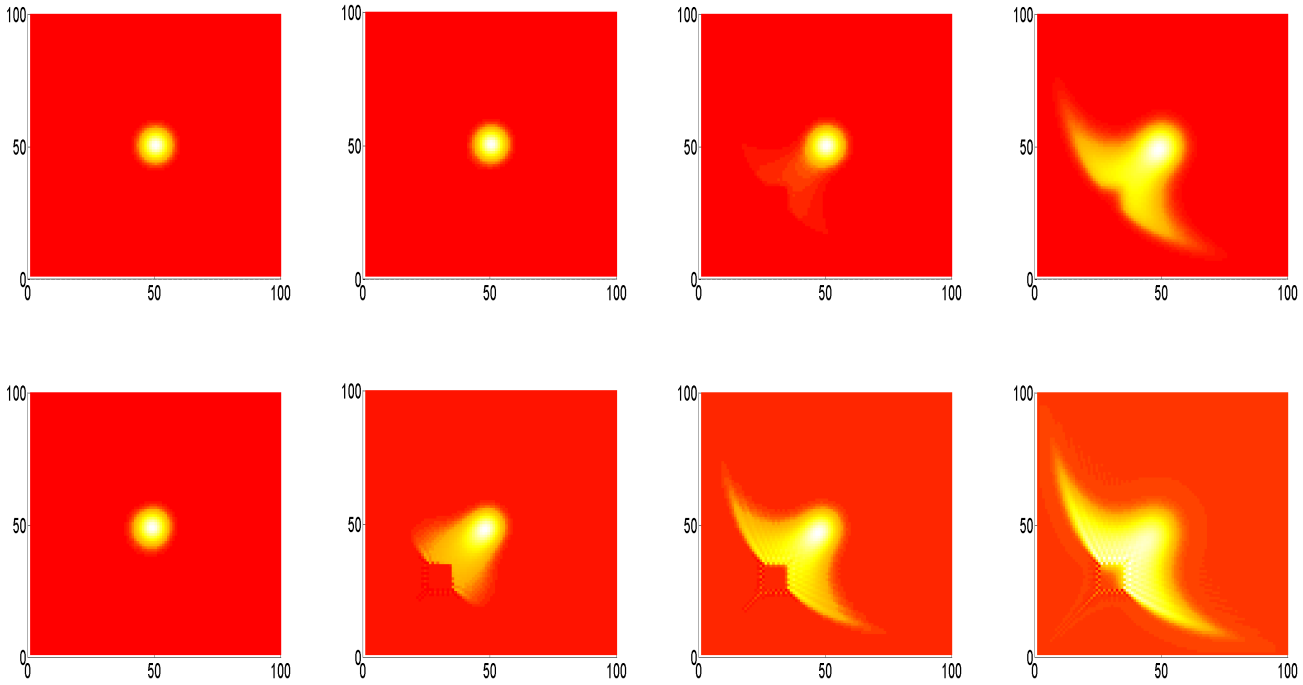

(a) Simulation time 50 (b) Simulation time 200 (c) Simulation time 1000 (d) Simulation time 5000

Fig. 4: Tissue Temperatures (top) and Blood Temperatures (below) at progressive simulation times

V. Conclusion

The model presented here represents only one stage in a larger mathematical system. Further work will involve the creation of a second model determining a quantitative measure of cell health and tissue integrity based upon a time-temperature history of the tissue subvolume. A third model will then be developed to close the loop which will link the spatially varying tissue integrity field to the physical properties used in the model presented here.

The results presented here are only solutions derived from numerical analyses. However, an analytical solution to (11) and (12) in nondimensional form with one-dimensional spatial derivatives has also been obtained. The authors are therefore also conducting a sensitivity analysis to determine the dominant behavioural terms and parameters. This is the subject of a parallel paper [5].

References

[1] H. Arkin, L. X. Xu, and K. R. Holmes, "Recent developments in modeling heat transfer in blood perfused tissues," *Biomedical Engineering, IEEE Transactions on*, vol. 41, no. 2, pp. 97–107, 1994.

[2] C. K. Charny, *Advances in Heat Transfer Bioengineering Heat Transfer*. San Diego: Academic Press, Inc., 1992, vol. 22, pp. 19–155.

[3] M. M. Chen and K. R. Holmes, "Microvascular contributions in tissue heat transfer." *Annals of the New York Academy of Sciences*, vol. 335, pp. 137–150, 1980.

[4] K. R. Diller, *Adcances in Heat Transfer Bioengineering Heat Transfer*. San Diego: Academic Press, Inc., vol. 22.

[5] T. Peng, D. P. O'Neill, and S. J. Payne : unpublished.

[6] H. H. Pennes, "Analysis of tissue and arterial blood temperatures in the resting human forearm," *J Appl Physiol*, vol. 85, no. 1, pp. 5–34, July 1998.

[7] S. Weinbaum and L. M. Jiji, "A new simplified bioheat equation for the effect of blood flow on local average tissue temperature." *Journal of biomechanical engineering*, vol. 107, no. 2, pp. 131–139, May 1985.

[8] L. Zhu, L. X. Xu, Q. He, and S. Weinbaum, "A new fundamental bioheat equation for muscle tissue–part ii: Temperature of sav vessels." *Journal of biomechanical engineering*, vol. 124, no. 1, pp. 121–132, February 2002.